

Hydrothermal synthesis of free-template zeolite T from kaolin

Sazmal E. Arshad, Eddy F. Yusslee, Md. Lutfur Rahman, Shaheen M. Sarkar, and Siti Z. Patuwan

Citation: [AIP Conference Proceedings](#) **1901**, 030004 (2017);

View online: <https://doi.org/10.1063/1.5010469>

View Table of Contents: <http://aip.scitation.org/toc/apc/1901/1>

Published by the [American Institute of Physics](#)

Hydrothermal Synthesis of Free-Template Zeolite T from Kaolin

Sazmal E. Arshad^{1, a)}, Eddy F. Yusslee^{1, b)}, Md. Lutfor Rahman^{1, c)},
Shaheen M. Sarkar^{2, d)} and Siti Z. Patuwan^{1, e)}

¹*Faculty of Science and Natural Resources, Universiti Malaysia Sabah, 88400 Sabah, Malaysia.*

²*Faculty of Industrial Sciences and Technology, Universiti Malaysia Pahang, 26600 Pahang, Malaysia*

^{a)}Corresponding author: sazmal@ums.edu.my,

^{b)}eddy@ums.edu.my,

^{c)}Lutfor73@gmail.com,

^{d)}shaheen@ump.edu.my,

^{e)}sitizubaidahpatuwan@gmail.com

Abstract. Free-template zeolite T crystals were synthesized via hydrothermal synthesis by utilizing the activated kaolin as silica and alumina source, with the molar composition of 1 SiO₂: 0.04 Al₂O₃: 0.26 Na₂O: 0.09 K₂O: 14 H₂O. Observation of the formation of free-template zeolite crystals were done at temperature 90 °C, 100 °C and 110 °C respectively. It was therefore determined that during the 120 h of the synthesis at 90 °C, zeolite T nucleated and formed a first competitive phase with zeolite L. As temperature increases to 100 °C, zeolite T presented itself as a major phase in the system at time 168 h. Subsequently, development of Zeolite T with second competitive phase of zeolite W was observed at temperature 110 °C. In this study, XRD and SEM instruments were used to monitor the behavior of zeolite T crystals with respect of temperature and time. By using natural resource of kaolin clay as a starting material, this paper hence aims to provide new findings in synthesis of zeolite T using low energy consumption and low production cost.

INTRODUCTION

The effect of global warming resulting from excessive emission of CO₂ in the atmosphere is an environmental problem that needs to be address critically. It is therefore considered as a significant challenge to provide an effective method in minimizing the greenhouse gases emissions as much as possible [1-3]. Fortunately, with ongoing research development fueled together with remarkable results, molecular sieve proves to possess an undeniable potential in selective removal of carbon dioxide [4-5]. Such exceptional result includes zeolite T, which has been introduced in early 1970 by Bennet and Gard [6]. Zeolite T is a unique new generation molecular sieve as it belongs to the intergrowth family of natural-occurring zeolite offretite and erionite [6-7]. Preparation of zeolite T by Mirfendereski and Mohammadi (2011) [8] was done in aqueous alkaline via hydrothermal synthesis where it is concluded that the crystallization condition of 1SiO₂: 0.04Al₂O₃: 0.26Na₂O: 0.09K₂O: 14H₂O is 120 °C at 168 h. The study also reported on the ability of zeolite T to develop alongside zeolite L and W. Other study by Yin *et al.*, (2015) [9] had also successfully synthesized zeolite T that aggregates at different sizes via hydrothermal synthesis. However, it was also found out that the free template sample prepared at 144 h for 100 °C has no crystalline phases. Therefore, they concluded that synthesis of zeolite T without using a template took 192 h to show crystalline peaks at XRD pattern.

Currently, zeolite T is being developed in membrane form in order to investigate its potential application. Cui *et al.*, (2004) [10] had reported that zeolite T membranes displayed excellent pervaporation performance for water/organic liquid mixtures and were practically stable in an acetic acid solution for the dehydration of organic liquids containing organic acid. More recently, CO₂ separation and adsorption using zeolite T material has attracted more attention due to their tunable chemical properties while also offering vast potential application in separation of gas/vapor/liquid to improve reaction conversion or product selectivity. In addition, development of a novel membrane

candidate for CO₂ separation by Yin *et al.*, (2013) [3] had brought them to a conclusion that zeolite T composite membrane also shows good CO₂ separation performance either in single permeation and equimolar mixed gases permeation (CO₂/CH₄ and CO₂/N₂). However, synthesis of zeolite T is usually conducted by using pure chemical such as colloidal silica, silica fume, precipitated silica, silica sol, colloidal silica and silicic acid as silica sources while alumina powder, aluminate powder, sodium aluminate and alkaline aluminate were used as alumina sources [3-5,9,11-12]. The utilization of natural resources of kaolin clay for zeolite T synthesis is a rare topic, even though the kaolin clay offers a wide potential silica-alumina source for zeolitization. Kaolin majorly consists of mineral from kaolinite which are made up from tetrahedral layer of silica alternating with an octahedral layer of alumina and linked by oxygen atom and hydroxyls [13]. Due to its makeup of 1:1 layer of silica/alumina, it is considered as a convenient component in the synthesis of zeolite. Nevertheless, since kaolin is considered as too stable to be reactive, thus, the transformation of kaolin into metakaolin via dehydroxylation is necessary [14].

Many researchers have successfully synthesized zeolite T as far as investigating the factors with regards to the preparation of zeolite T. In spite of that, with due respect to all knowledgeable researchers, zeolite T from the aspect of kaolin to metakaolin has not been investigated yet. Up to now, majority of the studies deal with pure chemicals to synthesize and prepare zeolite T rather than utilizing the natural resource of kaolin clay as the starting material. Therefore, the objectives of this study is to synthesize a free-template of zeolite T from the formulation of metakaolin as a silica-alumina source using low energy consumption, while also investigating the influence of temperature and time towards the hydrothermal synthesis, with the temperature ranging from 90 to 110 °C and time from 96 to 192 h. Synthesized zeolite T was determined using XRD and SEM respectively.

EXPERIMENTAL

Methods of Characterization and Determination in Synthesizing Zeolite T

Dehydroxylation of kaolin was determined by using the Thermal gravimetric analysis (TGA) to acquire a specific temperature of calcination of kaolin into metakaolin. Kaolin (~3 mg) was heated at parameters of 30 °C to 750 °C. Characterization of zeolite T was conducted, using X-ray diffraction analysis (XRD) built with Philips X'pert Pro PW 3040; PANalytical. Data collection was carried out in the range of 2 θ : 5 – 80°, step size of 0.02° under Cu K α = 1.54056, 30 mA and 40 kV. Crystal morphologies were studied by utilizing the Scanning electron microscope (SEM) – ZEISS, MA10 where the zeolite samples were coated with gold.

Preparation of Silica-Alumina Source

Brick-like colored kaolin powder was purchased from Sibelco Co. and had undergone heat treatment for dehydroxylation. Bulk powder was placed in a crucible pan and treated at 750 °C for 4 hours inside a muffle furnace.

Synthesis of Zeolite T

Zeolite T was synthesized by the following molar composition of 1SiO₂: 0.04Al₂O₃: 0.26Na₂O: 0.09K₂O: 14H₂O with a few modifications toward SiO₂/ Al₂O₃ sources. The 25 molar ratio of SiO₂/ Al₂O₃ in the system was obtained by the homogeneously mixed of metakaolin powder with silica fume. The homogenous powder was stored inside a Teflon bottle and capped tightly to avoid spillage of silica fume. The alkaline activator was freshly prepared consisting of sodium hydroxide, NaOH pellets and potassium hydroxide, KOH pellets. The mixtures were mixed together and was dissolved using 14 molar ratio of H₂O. The homogeneously alkaline medium was then poured into metakaolin-silica fume and was vigorously shaken. The Teflon bottle was left at orbital shaker overnight at maximum spinning speed of 250 rpm. Teflon bottle containing the homogenized mixture was then placed inside an oven at an elevated temperature and time. Table 1 shows the parameters in regards to the temperature and time that were elected for this study. All samples of zeolite T were filtered via vacuum suction and rinsed using excessive water (pH of 7) prior crystallization phase at 120 °C for 2 h inside an oven. Crystallized zeolite T were then stored inside a desiccator for characterization.

TABLE 1. Temperature and time elected for synthesizing zeolite T.

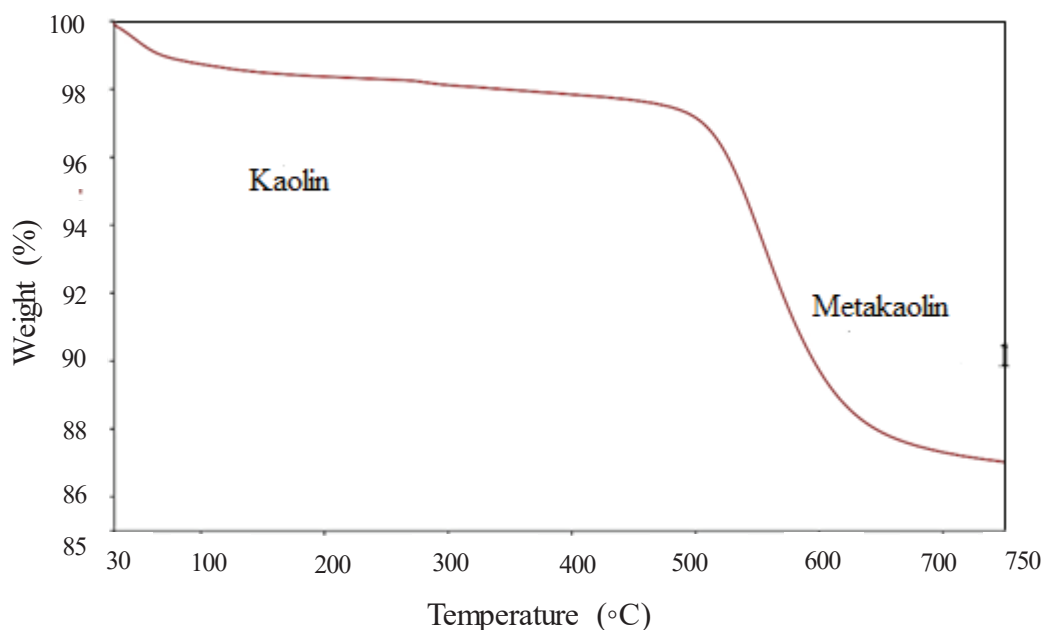
Temperature (°C)	Time, h	Crystallization
90	192	120 °C, 2 h
100	168	
110	144	
	120	
	96	

RESULTS AND DISCUSSION

Metakaolinization

Dehydroxylation of kaolin had causes 1:1 layer of silica tetrahedral sheet and the alumina octahedral sheet to experience a mass loss whereas four hydroxyl groups shared by alumina and silica layer transformed into a two water molecule which escaped from the layers of kaolinite [14-15]. Figure 1 shows the TGA curve of kaolin sample treated at a temperature range of 30 °C – 750 °C during thermal analysis. In Figure 1, it is observed that there is a weight loss curve of kaolin treated up to 750 °C for 4 hours. With 100% weight assigned at the starting temperature (30 °C), it is noted that as the temperature rose between 600 °C – 750 °C, the percentage of weight dropped from 100% to about 88% which indicated that dehydroxylation of kaolin into metakaolin has taken place.

Dehydroxylation of kaolin into metakaolin was then divided into three regions where it was determined that minor weight loss [14], started at temperature of 30 – 400 °C; followed by drastic weight drop at temperature of 400 – 600 °C. Finally, at 600 – 750 °C, kaolin lost about 12% of its weight during the calcination as shown in TGA curve at Figure 1. Therefore, due to the loss of hydroxyl groups in the form of water molecule, the crystal structure of kaolinite collapsed during reformation of amorphous phase of metakaolinite. Figure 2 shows the XRD patterns of both kaolin and metakaolin that were used in this study. The commercialized kaolin powder shows strong significant peaks of kaolinite at the value of 2 θ 12.29°, 24.87°, 34.95°, 35.99° and 38.36° but disappeared after calcination indicated the transformation of kaolin into metakaolin. Metakaolin is maintained at the *a* and *b* kaolinite lattice parameters while *c*-axis vanished; which deduced that metakaolin is an amorphous material [16].

**FIGURE 1.** TGA curve of dehydroxylation of kaolin into metakaolin calcined at 750 °C for 4 hours.

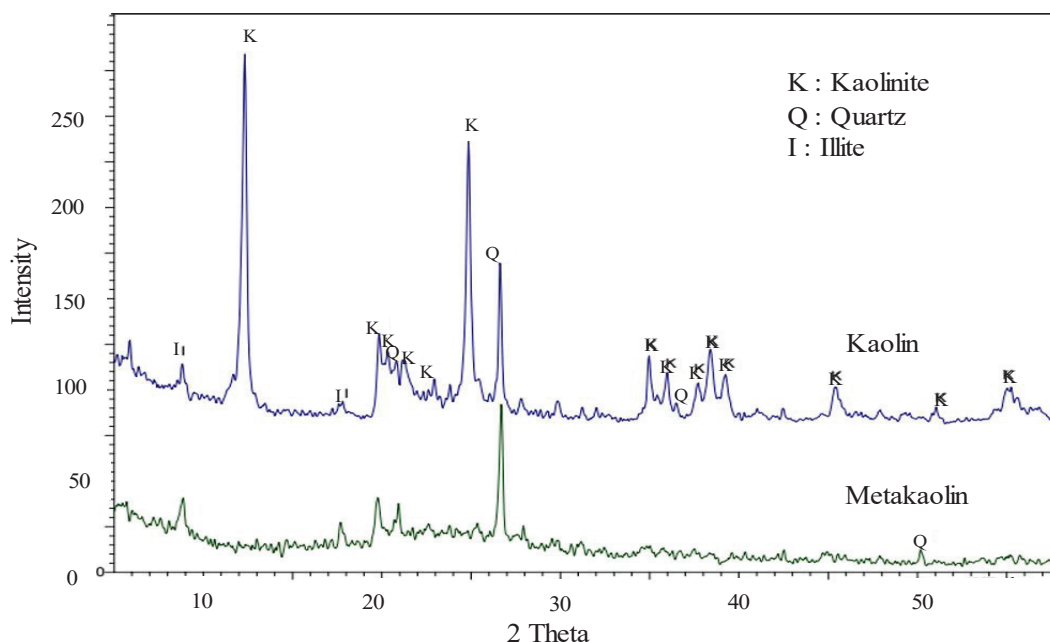


FIGURE 2. XRD diffractogram of dehydroxylation of kaolin into metakaolin calcined at 750 °C for 4 h.

Zeolite T from Metakaolin

Hydrothermal Synthesis at 90 °C, 100 °C, and 110 °C

Figure 3 shows the x-ray diffractograms of zeolite T samples crystallized at different times. Crystallization peak of zeolite T at 96 h were at the minimum intensity where the value of 2θ corresponding to zeolite T only existed at 19.35° and 23.64° . However, a sample synthesized at 96 h shows strong nucleation of zeolite L as a major species while zeolite T a minor. Strong peaks of zeolite L were spotted at the value of 2θ , 5.53° , 22.63° , 28.03° and 30.67° . Meanwhile, as the temperature was constant and synthesis time increased to 120 h, synthesized zeolite sample showed significant peaks of the zeolite T at 2θ of 7.68° (58%), 19.30° (39.16%), 20.43° (49.69%) and 23.61° (79.82%). Nucleation of zeolite T for samples synthesized at 90 °C showed positive progress as the time increased steadily. Meanwhile at 144 h, peaks of zeolite T intensified and increased slightly significantly at 2θ of 7.71° (73.49%), and 23.71° (94.85%).

Despite the favorable growth of zeolite T crystals, co-existing species of zeolite L also arose along. The growth of zeolite T – zeolite L were developed as major phase at 2θ of $\pm 5.59^\circ$ ($I_0 = 100\%$) as time was prolonged to 120 h until 192 h. Despite the convenient growth of zeolite L as the synthesis time increased at the temperature of 90 °C, nucleation of zeolite T is also observed to develop actively in conjunction with the significant crystallization of zeolite L which remained significant at the time 96 h – 192 h. Figure 4 shows the crystal morphologies of zeolite T rod-like shape along with zeolite L at 90 °C with different time intervals. Figure 4 (a) shows sample prepared at time 96 h, where only the crystals of zeolite L monopolized the system. Meanwhile, Figure 4 (b) shows the zeolite T crystals in rod-like shape obtained at time 192 h.

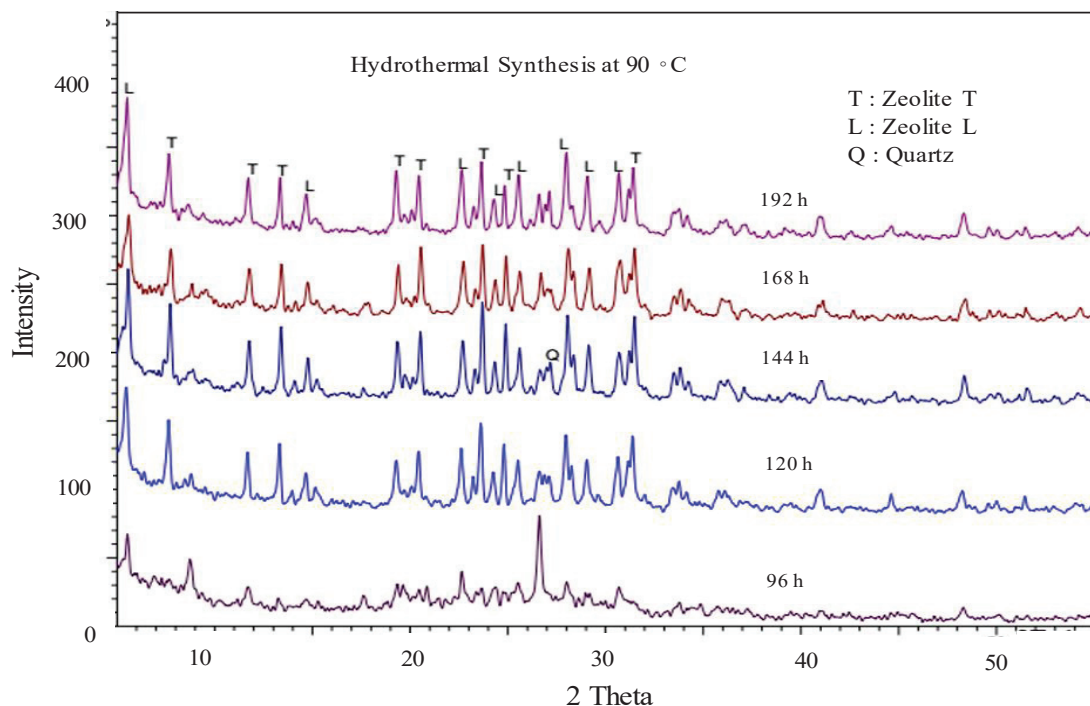


FIGURE 3. XRD diffractograms of samples prepared at 90 °C for 96 h, 120 h, 144 h, 168 h and 192 h respectively, where T: Zeolite T, L: Zeolite L and Q: Quartz.

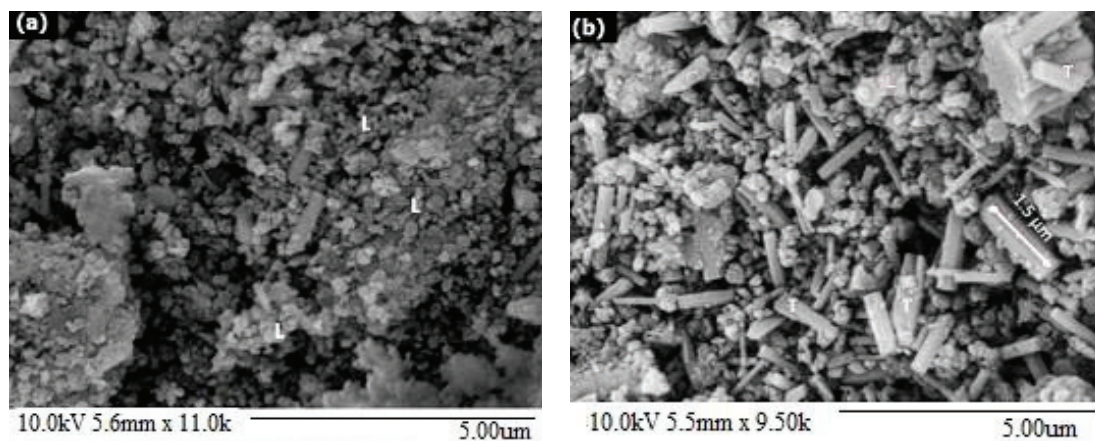


FIGURE 4. SEM morphologies of samples prepared at 90 °C for (a) 96 h and (b) 192 h respectively.

Samples synthesized at temperature of 100 °C at different times resulted in the zeolite T having different purity level as shown in the XRD diffractograms (Figure 5). At 96 h, zeolite T crystals developed with zeolite L is observed to develop as a major phase in the system. As the synthesis parameters were prolonged at 120 h and 144 h – crystallinity of both zeolite T and L increased steadily. At both elevated time, peaks of zeolite L only dominated at value 2θ of 5.5° and this peak intensified from the time of 96 h until 144 h while other peaks corresponding to zeolite L (2θ : $\pm 14.6^\circ$, $\pm 22.66^\circ$ and $\pm 29.10^\circ$) remained the same throughout the synthesis. As a consequence, 96 h to 144 h treated samples results in having zeolite L as a major phase instead of zeolite T.

However, samples that were synthesized at 168 h showed that the growth of zeolite T is slightly above the peak of zeolite L (2θ : 5.5° with I_0 : 93.5 %). During the parameter study of temperature of 100 °C in 168 h, zeolite T develops

as a major species at the value of 2θ at 7.69° (I_0 : 100%), 19.38° (I_0 : 31.4 %), 23.66° (88.96 %) and 24.82° (I_0 : 58.44 %), which corresponded with peaks of zeolite T. Samples synthesized at 100°C for 168 h showed the development of zeolite T as a major phase but as the time was extended towards 192 h, crystallinity of zeolite T at 2θ of 7.67° dropped with I_0 of 75.57 % while crystallinity of zeolite L at 2θ of 5.52° slightly dropped with I_0 of 92.84 %. This showed that crystallization of zeolite T and zeolite L within the system of zeolite T is strongly affected by time which consequently corresponds to different range of temperature. Figure 6 shows the morphologies of zeolite T prepared at 100°C for (a) 168 h and (b) 192 h. At 168 h, zeolite T crystallized in a size of $2\ \mu\text{m}$ while at 192 h, zeolite T crystals are $2.5\ \mu\text{m}$ in size with uneven crystals formation.

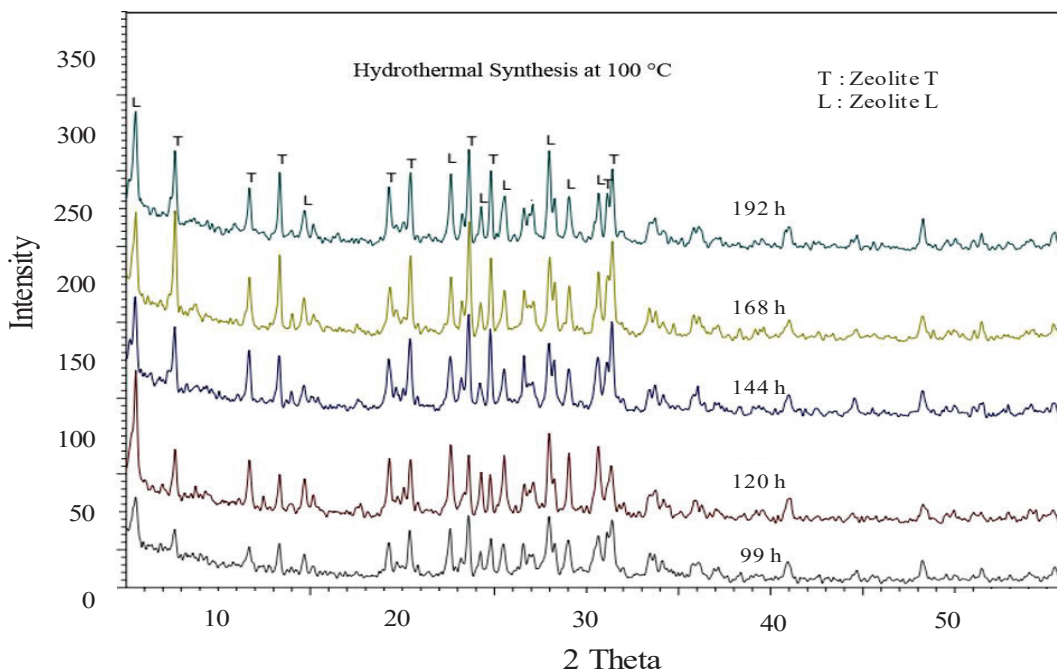


FIGURE 5. XRD diffractograms of samples prepared at 100°C for 96 h, 120 h, 144 h, 168 h and 192 h respectively, where T : Zeolite T and L : Zeolite L.

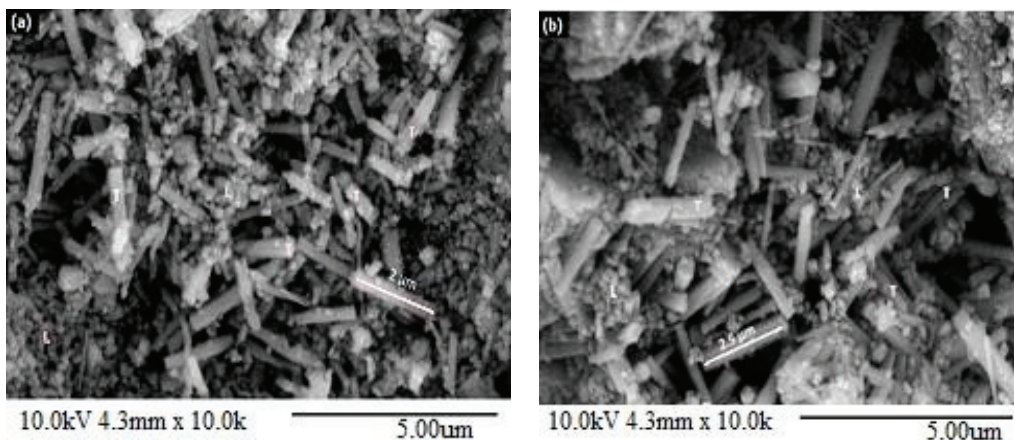


FIGURE 6. SEM morphologies of samples prepared at 100°C for (a) 168 h and (b) 192h respectively.

Figure 7 shows XRD diffractograms for all samples prepared at the temperature of 110°C at different times. Samples synthesized at 110°C differs from samples prepared at the temperature of 90°C and 100°C , since zeolite T develops not only with zeolite L but also with zeolite W. Samples prepared at the time of 96 h and 120 h did not show the presence of zeolite W whereas zeolite T showed peaks at 2θ of $\pm 7.69^\circ$ at I_0 of 31.64 % (96 h) and 81.26 % (120

h). Zeolite L on the other hand showed peaks at 2θ of $\pm 5.50^\circ$ at I_0 of 100 % for both times. The nucleation of zeolite W occurred as the samples were synthesized at 144 h until 192 h. At a time of 144 h, zeolite T showed peaks at 2θ of 7.71° (I_0 : 51.07%), 19.31° (I_0 : 40.69 %) and 23.66° (I_0 : 92.31 %). Subsequently, zeolite L showed peaks at 2θ of 5.59° (I_0 : 47.3 %) and 22.70° (I_0 : 45.55 %) while zeolite W was at 2θ of 28.04° (I_0 : 75.01 %) and 30.75° (I_0 : 39.4 %).

Meanwhile, at the synthesis time of 168 h, zeolite T crystallized slightly lower than the previous time where it peaked at 2θ of 7.70° (I_0 : 30.95%), 19.31° (I_0 : 47.74 %) and 23.66° (I_0 : 64.91 %), as opposed to crystal of zeolite L and zeolite W that dominate the system. As the temperature remains constant and the time was increased to 192 h, zeolite T crystallized no further than the previous sample while zeolite W served as a major phase in the system. Morphologies by SEM at Figure 8 shows that the crystals of zeolite T evolved into zeolite L and at time of 192 h, zeolite T were covered by crystals of zeolite W. Subsequently, at time of 120 h, zeolite T formed is $2.5 \mu\text{m}$ in size where it grows along with the crystals of zeolite T. As the time increased to 144 h, zeolite W nucleated while zeolite T re-dissolved into the system until it totally disappeared at time of 192 h.

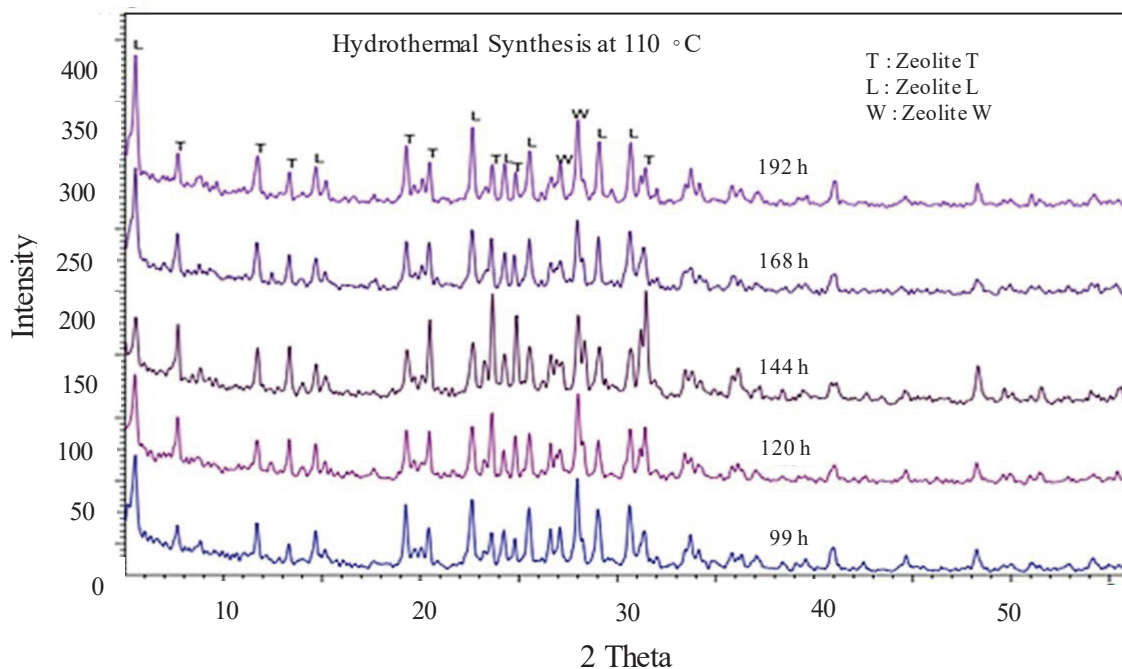


FIGURE 7. XRD diffractograms of samples prepared at 110 °C for 96 h, 120 h, 144 h, 168 h and 192 h respectively, where T : Zeolite T, L : Zeolite L and W: Zeolite W.

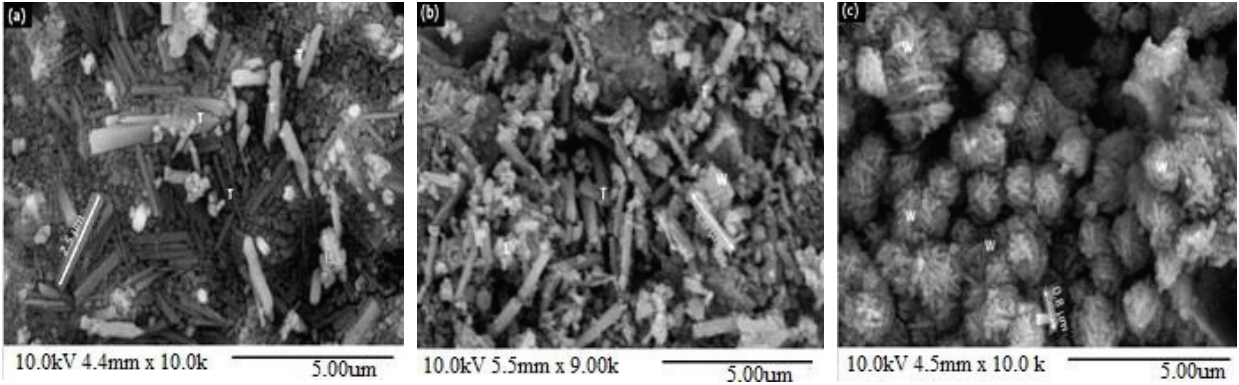


FIGURE 8. SEM morphologies of samples prepared at 110 °C for (a) 120 h, (b) 144 h and (c) 192 h respectively.

Effect of Time and Temperature

Crystallization of zeolite T were strongly affected by temperature and time as zeolite T evolved easily into zeolite L and zeolite W [4-5]. Table 2 which shows the synthesis condition towards crystallization of the major species indicated that the formation of zeolite T from metakaolin generated zeolite L and W in the system, while its dominance were controlled by temperature and time. Zeolite T-, L- and W- are coexisting type zeolites [17-22] and due to this factor their structures are closely identical to each other, resulting in variable crystal-distribution yields within 144 h synthesized samples. In addition, important information was added in Table 2 for future references regarding the synthesis of either zeolite T, zeolite L or zeolite W. From this study, it is found out that Zeolite L can be prepared at temperature 90 °C, followed by temperature of 100 °C for zeolite T and 110 °C for zeolite W. Definite temperature and time variation in this study shows that the crystallization of zeolite from metakaolin has minimize the requirement of temperature and time for the synthesis of zeolite materials with respect of previous literatures [3,5,11].

Due to the high temperature (highest temperature for this study was 110 °C) and prolonged time (144 h – 192 h), the strong crystallization of zeolite T (100 %) from temperature of 100 °C and time of 168 h decreases and shifted to zeolite L; followed by the formation of zeolite W at temperature 110 °C. This indicates that the temperature of 110 °C is more than needed for the formation of zeolite T crystals; which in turn also causes the formation of zeolite L and initiated the growth of zeolite W.

TABLE 2 Phase evolution of zeolite crystals from metakaolin affected by temperature and time.

Time	Phase(s) for different temperatures, °C		
	90	100	110
96	Majority : L Minority: T	Minority: L and T	Majority : L Minority: T and W
120	Majority : L Minority: T	Majority : L Minority: T	Majority : L Minority: T and W
144	Majority : T and L	Majority : T and L	Majority : T , L and W
168	Majority : T and L	Majority: T (100 %) Minority: L	Majority : L and W Minority: T
192	Majority : L Minority: T (minimum)	Majority : T and L	Majority : W Minority: T and L

CONCLUSIONS

Zeolite T crystals were prepared from metakaolin via hydrothermal method while the effects of temperature and time towards the crystallization of zeolite T were investigated. XRD patterns and SEM morphologies gave evidences that treatment at 100 °C for 168 h is the adequate parameters to yield zeolite T with molar composition of 1SiO_2 : $0.04\text{Al}_2\text{O}_3$: $0.26\text{Na}_2\text{O}$: $0.09\text{K}_2\text{O}$: $14\text{H}_2\text{O}$ as a major phase in the system. Synthesis of zeolite T from metakaolin was also found out to begin nucleating at 90 °C for 120 h, which is the lowest temperature that has ever been reported.

ACKNOWLEDGEMENTS

This study was supported by the project grant of RAG-0068-SG-2015 funded by Universiti Malaysia Sabah, Malaysia.

REFERENCES

1. X. Yu, Z. Wang, H. Wei, J. Yuan, J. Zhan, X. Wang and S. Wang, *J. Membrane Sci.* **362**, 265-278 (2010).
2. L. Zhao, E. Riensche, R. Menzer, L. Blum and D. Stolten, *J. Membrane. Sci.* **325**, 284-294 (2008).
3. X. Yin, N. Chu, J. Yang, J. Wang and Z. Li, *Int. J. Greenhouse Gas. Cont.* **15**, 55-64 (2013).
4. M. Mirfendereski, T. Mazaheri, M. Sadrzade and T. Mohammadi, *Sep. Purif. Technol.* **61**, 317-323 (2008).
5. M. Rad, S. Fatemi and M. Mirfendereski, *Chem. Eng. J.* **90**, 1687-1695 (2012).
6. R. Gorrng, *J. Catal.* **31**, 13-26 (1973).
7. R. Zhou, S. Zhong, X. Lin and N. Xu, *Microporous Mesoporous Mater.* **124**, 117-122 (2009).
8. M. Mirfendereski and T. Mohammadi, *Powder Technol.* **206**, 345-352 (2011).
9. X. Yin, Z. Li, S. Wang, N. Chu, J. Yang and J. Wang, *Microporous Mesoporous Mater.* **201**, 247-257 (2015).
10. Y. Cui, H. Kita and K. Okamoto, *J. Mater. Sci.* **236**, 17-27 (2004).
11. Q. Jiang, J. Rentschler, G. Sethia, S. Weinman, R. Perrone and K. Liu, *Chem. Eng. J.* **230**, 380-388 (2013).
12. Y. Y. Zee, C. Siang-Piao, W. Z. Peng and Mohamed, A. B, *Microporous Mesoporous Mater.* **197**, 79-88 (2014).
13. H. Murray, H. H. 2006. Chapter 2: Structure and composition of the clay minerals and their physical and chemical properties. In Haydn, H. M. (ed.). *Developments in Clay Science*, Volume 2, pp 7-31. Elsevier.
14. E. B. Johnson, Sazmal and E. Arshad, *App. Clay. Sci.* **97-98**, 215-221 (2014).
15. R. Wardle, G. Brindley, *Am. Min.* **57**, 5-6, 732 (1972).
16. G. Brindley and M. Nakahira, *J. Amer. Cera. Soc.* **42**, 314-418 (1959).
17. S. Yong and S. Wha, *Powder Technol.* **145**, 10-19 (2004).
18. L. Yun-Jo, S. Jin and B. Kyung, *Microporous Mesoporous Mater.* **80**, 237-246 (2005).
19. J. White, P. Dutta, K. Shqau and H. Verweji, *Microporous Mesoporous Mater.* **115**, 389-398 (2008).
20. J. Cejka, H. Van Bakkum, A. Corma and F. Schüth, (2007). *Introduction to zeolite science and practice, in studies in surface science and catalysis 168* (p. 525). Elsevier BV Amsterdam, Neth.
21. T. Nagase, Y. Kiyozumi, Y. Nemoto, N. Hirano, Y. Hasegawa, T. Ikeda, T. Inoue, T. Nishide and F. Mizukami, *Microporous Mesoporous Mater.* **126**, 107-114 (2009).
22. S. Yeong-Hui, P. Eko Adi, J. Nanzhe, O. Soon-Moon and P. Sang-Eon, *Microporous Mesoporous Mater.* **128**, 108-114 (2010).